Early version, also known as pre-print

Link to publication record in Explore Bristol Research
PDF-document

University of Bristol - Explore Bristol Research
General rights

STRUCTURAL STABILITY OF THE TWO-FOLD SINGULARITY

S. FERNÁNDEZ-GARCÍA*
D. ANGULO GARCÍA, G. OLIVAR TOST†
M. DI BERNARDO‡
M. R. JEFFREY§

Abstract. At a two-fold singularity, the velocity vector of a flow switches discontinuously across a codimension one *switching manifold*, between two directions that both lie tangent to the manifold. Particularly intricate dynamics arises when the local flow curves towards the switching manifold from both sides, a case referred to as the Teixeira singularity. The flow locally performs two different actions: it winds around the singularity by crossing repeatedly through, and passes through the singularity by sliding along, the switching manifold. The case when the number of rotations around the singularity is infinite has been analysed in detail. Here we study the case when the flow makes a finite – but previously unknown – number of rotations around the singularity between incidents of sliding. We show that the solution is remarkably simple: the maximum and minimum number of rotations made anywhere in the flow differs only by one, and increases incrementally with a single parameter: the angular jump in the flow direction across the switching manifold, at the singularity.

Key words. Filippov, Teixeira, singularity, discontinuity, sliding

AMS subject classifications. 34C23, 37G10, 37G35

1. Introduction. Piecewise-smooth dynamical systems continue to find increasing application in modelling stick-slip and impact in rigid body mechanics, switching in electrical control circuits and robotics, temperature dynamics in the phase transitions of superconductors, as well as numerous other biophysical, ecological and industrial problems; see for example [1, 2, 4, 7, 11, 14, 15]. Any of these contain examples of piecewise-smooth systems of the general class discussed here, namely three dimensional flows whose time derivative is discontinuous across a hypersurface or *switching manifold*, while the flow itself is continuous.

Two-fold singularities in such systems were first described by Filippov [6]. At a two-fold, the flow lies tangent to both sides of the switching manifold, but its magnitude and direction tangent to the manifold are discontinuous. Filippov highlighted the fact that, while two-folds should appear under generic conditions, one particular type seemed to be structurally unstable, meaning that any small change to its description would result in qualitatively different dynamics. In this case, the flow curves towards the switching manifold from both sides, as depicted in figure 1.1. Intrigue grew with Teixeira's continued study of its structural and asymptotic stability [12], and this case became known as the *Teixeira singularity*. The difficulties of marrying the two-fold's genericity with its structural instability, and the realisation that the two-fold provides a route to robust non-deterministic dynamics [3], create a need to

understand its possible role in applications. This, in turn, requires a few gaps in the classification of its dynamics to be filled.

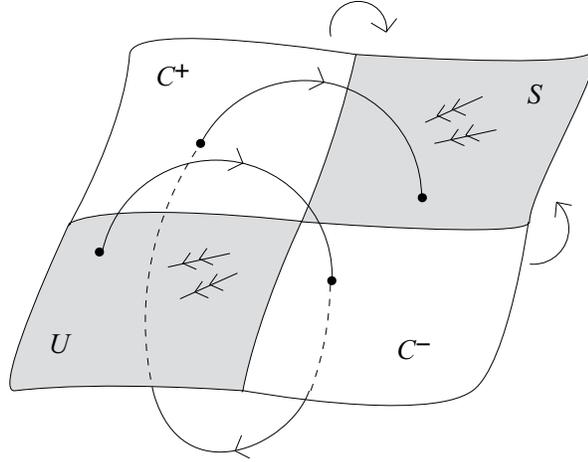Through [6, 9, 12], various structurally stable classes of Teixeira singularity, and the bifurcations between different classes, were identified, leading to a detailed picture of the local dynamics. The singularity is never a global attractor or repeller, but rather a two-way channel between disjoint domains in which the switching manifold attracts or repels the surrounding flow, and around which the flow can wind, sometimes intricately.

Yet there remains a missing piece in the puzzle of the Teixeira singularity's structural stability. It was shown in [9] that the local dynamics depends crucially upon a single quantity: the jump in the flow's direction through the switching manifold at the singularity. This jump determines whether the flow winds around the Teixeira singularity "at most once", "at least once", or "infinitely many times", between instances of sliding. The topological stability of these classes under perturbation was described in [3]. The remaining obstruction to fully establishing the stable topologies of the two-fold lies in the phrase "at least once". In what manner does the number of rotations increase from one to infinity? Does this take place through a series of well defined bifurcations, between which structural stability is restored? Do regions of existence for different rotation numbers overlap? And so on.

The vector field in a sufficiently small neighbourhood of the Teixeira singularity is approximated by a normal form now familiar from [3, 6, 9, 12] (the validity of which can also be seen in examples simulated in [3]). For this local model, we show here that the number of rotations the flow makes around the singularity can be expressed in a closed form. It depends on a single parameter, namely the angle through which the flow jumps across the switching manifold. We equate a ratio of the tangents of the angles between the flow's direction and the two folds at the singularity, to a function $\cos^2 \frac{\pi}{r+1}$, where $r > 1$. Then the number of times any orbit in the flow crosses the switching manifold is given by $k = r$ when r is an integer, or by the integers k and $k + 1$ either side of r otherwise. Any number of crossings k corresponds to the flow

making $(k+1)/2$ rotations around the singularity between visits to the sliding regions.

The paper is set out as follows. In section 2 the Teixeira singularity is defined. In section 3 we classify its local dynamics using previous results, and add a Theorem regarding rotation numbers in the flow. In section 4 we recall the local normal form, and derive its dynamics in the Filippov convention in section 5. In section 6 we prove the main Theorem and its Corollary, and illustrate the results with some simulations in section 7, with some concluding remarks in section 8.

2. The Teixeira singularity. For some variable $\mathbf{x} \in \mathbb{R}^3$ changing with time t, let the velocity vector $d\mathbf{x}/dt$ take different values $\partial_{t+}\mathbf{x}$ or $\partial_{t-}\mathbf{x}$ depending on the sign of some smooth scalar function $h(\mathbf{x})$. This defines a piecewise-smooth flow along which the time derivative operator can be written as

$$(2.1) \qquad \frac{d}{dt} = \begin{cases} \partial_{t+} & \text{if} \quad h(\mathbf{x}) > 0, \\ \partial_{t-} & \text{if} \quad h(\mathbf{x}) < 0, \end{cases}$$

and the surface $h = 0$ is called the *switching manifold*. The operators $\partial_{t\pm}$ are Lie derivatives along smooth flows either side of $h(\mathbf{x}) = 0$, introduced in more depth in the Appendix.

A *two-fold singularity* is defined as a point $\hat{\mathbf{x}}$ where,

$$(2.2) \qquad h(\hat{\mathbf{x}}) = \partial_{t+}h(\hat{\mathbf{x}}) = \partial_{t-}h(\hat{\mathbf{x}}) = 0,$$

subject to non-degeneracy conditions

$$(2.3) \qquad \partial_{t\pm}^2 h(\hat{\mathbf{x}}) \neq 0,$$
$$(2.4) \qquad \det\left[\partial_{\mathbf{x}}h(\hat{\mathbf{x}}),\ \partial_{\mathbf{x}}\partial_{t+}h(\hat{\mathbf{x}}),\ \partial_{\mathbf{x}}\partial_{t-}h(\hat{\mathbf{x}})\right] \neq 0,$$

where $\partial_{\mathbf{x}}$ is the gradient operator with respect to $\mathbf{x}$. These conditions are discussed in [3, 6, 9, 12], but let us briefly review how they lead to the geometry in figure 1.1. A *fold* is a set of points that satisfy $\partial_{t+}h(\mathbf{x}) = h(\mathbf{x}) = 0$ or $\partial_{t-}h(\mathbf{x}) = h(\mathbf{x}) = 0$, meaning the flow is tangent to the switching manifold from above or below respectively, and such points form curves on the switching manifold. Non-degeneracy conditions $\partial_{t+}^2 h \neq 0$ or $\partial_{t-}^2 h \neq 0$ (attached to $\partial_{t+}h = 0$ or $\partial_{t-}h = 0$ respectively) ensure that the order of the tangency is quadratic, and not higher. Therefore (2.2) defines a point where the flow is tangent to *both* sides of the switching manifold simultaneously, while condition (2.3) ensures these are *both* of quadratic order. The point $\hat{\mathbf{x}}$ therefore lies at the intersection of two curves of folds, and condition (2.4) ensures that the intersection is transversal.

The flow's local curvature is characterized by the second Lie derivatives of h. In particular, the dynamics at a two-fold depends critically upon two quantities,

$$(2.5) \qquad v^+ = \frac{\partial_{t+}\partial_{t-}h(\hat{\mathbf{x}})}{\sqrt{-(\partial_{t+}^2 h(\hat{\mathbf{x}}))(\partial_{t-}^2 h(\hat{\mathbf{x}}))}}, \quad v^- = \frac{-\partial_{t-}\partial_{t+}h(\hat{\mathbf{x}})}{\sqrt{-(\partial_{t+}^2 h(\hat{\mathbf{x}}))(\partial_{t-}^2 h(\hat{\mathbf{x}}))}}.$$

A Teixeira singularity is a specific type of two-fold where the flow curves towards the switching manifold from both sides, meaning that the second Lie derivatives satisfy

$$(2.6) \qquad \partial_{t+}^2 h(\hat{\mathbf{x}}) < 0 < \partial_{t-}^2 h(\hat{\mathbf{x}}),$$

therefore $v^{\pm}$ are real-valued and finite.

To study the dynamics of a flow with time derivative (2.1), it is necessary to extend this expression to the switching manifold, $h(\mathbf{x}) = 0$. A general method of restoring continuity at $h = 0$ was given by Filippov [6]. A convex combination of $\partial_{t\pm}$ provides a differential inclusion,

$$(2.7) \qquad \frac{d}{dt} \in \partial_{t^\lambda} = \lambda \partial_{t+} + (1 - \lambda)\partial_{t-}, \quad \lambda \in \begin{cases} 1 & \text{if} \quad h(\mathbf{x}) > 0, \\ [0,1] & \text{if} \quad h(\mathbf{x}) = 0, \\ 0 & \text{if} \quad h(\mathbf{x}) < 0. \end{cases}$$

It is then possible to define a flow along which the time derivative is given everywhere by (2.7), for some λ. The flow through any given point is continuous, but not necessarily unique, some consequences of which are explored in [3, 8] but are not of concern here.

3. Dynamical classification: the role of $v^\pm$. Fortunately, analysing the dynamics of the Teixeira singularity is simpler than considering the differential inclusion (2.7), and reduces to two kinds of dynamics at the switching manifold, sliding (shaded regions in figure 1.1) and crossing (unshaded regions in figure 1.1). At a point where

$$(3.1) \qquad (\partial_{t+}h(\mathbf{x}))(\partial_{t-}h(\mathbf{x})) > 0 \qquad \text{and} \qquad h(\mathbf{x}) = 0,$$

the component of the flow velocity normal to the switching manifold, $\partial_{t^\lambda}h(\mathbf{x})$, has the same sign for all λ as given by (2.7). The flow is then said to *cross* the switching manifold (giving the regions $C^\pm$ in figure 1.1). If the velocity normal to $h = 0$ changes direction across the switching manifold,

$$(3.2) \qquad (\partial_{t+}h(\mathbf{x}))(\partial_{t-}h(\mathbf{x})) < 0 \qquad \text{and} \qquad h(\mathbf{x}) = 0,$$

then (2.7) admits a velocity vector $\partial_{t^s}\mathbf{x} \in \partial_{t^\lambda}\mathbf{x}$, given by

$$(3.3) \qquad \partial_{t^s} = \frac{\partial_{t-}h}{(\partial_{t-} - \partial_{t+})h}\partial_{t+} + \left(1 - \frac{\partial_{t-}h}{(\partial_{t-} - \partial_{t+})h}\right)\partial_{t-},$$

that lies tangent to the manifold. This defines a flow that *slides* along the switching manifold. Since $\partial_{t+}h$ and $\partial_{t-}h$ do not vanish by (3.2), the flow from outside the switching manifold reaches or departs the sliding regions in finite time (defining the regions S and U respectively in figure 1.1). The attracting regions (where $\partial_{t+}h < 0 < \partial_{t-}h$) are known as *stable sliding*, and the repelling regions (where $\partial_{t-}h < 0 < \partial_{t+}h$) as *unstable sliding* (sometimes called 'escaping').

Thus the switching manifold is divided into regions of crossing given by (3.1), and regions of sliding given by (3.2). In [9] the following was proven with regard to sliding dynamics.

Theorem 1 *In the sliding regions local to the Teixeira singularity,*
- *(i) a unique orbit passes from unstable sliding to stable sliding if $v^+ > 0$ or $v^- > 0$;*
- *(ii) a unique orbit passes from unstable sliding to stable sliding if $v^\pm < 0$ and $v^+v^- < 1$;*
- *(iii) every orbit passes from stable sliding to unstable sliding if $v^\pm < 0$ and $v^+v^- > 1$;*

and in each of $(i) - (iii)$, passage between sliding regions is made directly via the singularity (i.e. without leaving the switching manifold).

The phase portraits responsible for this are shown in the shaded regions in figure 3.1(b), but since sliding is not the main concern of this paper we will not discuss these in detail. The following was also proven in [9] concerning crossing dynamics.

Theorem 2 *Between visits to the sliding regions, local to the Teixeira singularity, every orbit crosses the switching manifold:*

    (i) at most once from $h < 0$ to $h > 0$ if $v^+ > 0$, and
       at most once from $h > 0$ to $h < 0$ if $v^- > 0$;
    (ii) at least once if $v^\pm < 0$ and $v^+ v^- < 1$;
    (iii) infinitely many times if $v^\pm < 0$ and $v^+ v^- > 1$.

The number of crossings given by this theorem are illustrated in figure 3.1(a), forming a classification in the space of parameters $v^\pm$. In the unshaded regions in figure 3.1(b), phase portraits are shown that depict the return maps generated by the flow through the crossing regions.

Theorem 1 case (ii) inhabits the shaded region in figure 3.1(a), where the exact number of crossings for any given $v^\pm$ has not previously been described. As we show in section 6, this is resolved by the following theorem (the normal form referred to below will be described in section 4):

Theorem 3. *If $v^+ v^- = \cos^2 \frac{\pi}{k+1}$ where $k \geq 2$ is an integer, and $v^\pm$ are negative, then between visits to the sliding regions in the Teixeira singularity normal form system, any orbit crosses the switching manifold exactly k times.*

Corollary *to Theorem 3. If $v^+ v^- = \cos^2 \frac{\pi}{r+1}$ and $r > 1$ is not an integer, and $v^\pm$ are negative, then between visits to the sliding regions in the Teixeira singularity normal form:*

    1. any orbit crosses the switching manifold either k or $k+1$ times, where k and $k+1$ are the integers either side of r; and
    2. in normal form coordinates $\mathbf{x} = (x, y, z)$ where $x = 0$ is the switching manifold, on which $y = 0$ and $z = 0$ are the folds, the number of crossings made by a solution passing through a point $(0, y_0, z_0)$ changes across four lines, given by $y_0 = 0$, $z_0 = 0$, $z_0 = y_0 \Gamma^+_{(k+1)/2}$, and $y_0 = z_0 \Gamma^-_{(k+1)/2}$, in terms of functions

$$\Gamma^\pm_m = v^\pm / G_m(\arccos \sqrt{v^+ v^-}),$$
$$\text{and} \qquad G_m(\theta) = \sin\left([2m - 1]\theta\right) \cos\theta / \sin(2m\theta).$$

4. Local normal form. The derivative (2.1) defines a flow whose velocity is expressible as

$$(4.1) \qquad \frac{d}{dt}\mathbf{x} = \begin{cases} \mathbf{f}^+(\mathbf{x}) & \text{if} \quad h(\mathbf{x}) > 0, \\ \mathbf{f}^-(\mathbf{x}) & \text{if} \quad h(\mathbf{x}) < 0, \end{cases}$$

where $\mathbf{f}^\pm : \mathbb{R}^3 \mapsto \mathbb{R}^3$ are smooth, and $\mathbf{f}^\pm = \partial_{t\pm} \mathbf{x}$ or $\partial_{t\pm} = \mathbf{f}^\pm \cdot \partial_{\mathbf{x}}$.

The local dynamics can be studied almost entirely in the switching manifold, so it is useful to choose the first coordinate of $\mathbf{x}$ such that the switching manifold is given by $x = 0$. The two other coordinates, say y and z, can be chosen so that $\partial_{t+} h(\mathbf{x})$ and $\partial_{t-} h(\mathbf{x})$ vanish at $y = 0$ and $z = 0$ respectively, giving a local normal form for the Teixeira singularity (2.2) with a vector field (4.1) in which

$$(4.2) \qquad h(\mathbf{x}) = x, \qquad \mathbf{f}^+(\mathbf{x}) = \begin{pmatrix} -y \\ 1 \\ v^+ \end{pmatrix}, \qquad \mathbf{f}^-(\mathbf{x}) = \begin{pmatrix} z \\ v^- \\ 1 \end{pmatrix},$$
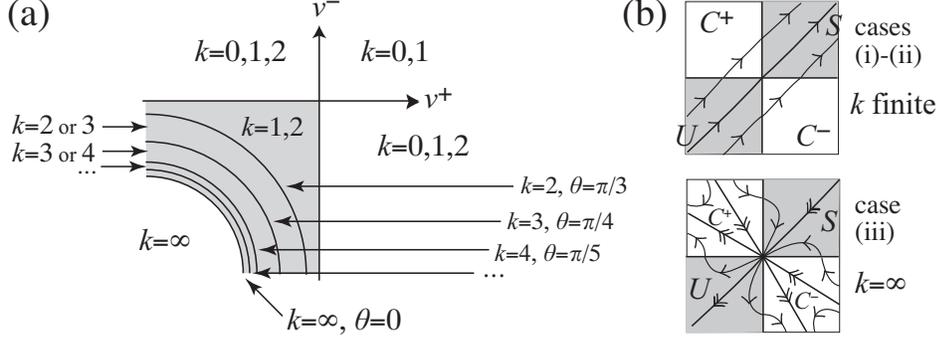
FIG. 3.1. Bifurcation diagram of the Teixeira singularity, showing: (a) k, the number of times any orbit crosses the switching manifold for different $v^{\pm}$; and (b) the corresponding phase portraits of the crossing maps (in crossing regions $C^{\pm}$) and sliding flow (in sliding regions S [stable] and U [unstable], shaded). This paper concerns the shaded region in (a). On each of the curves $v^{+}v^{-} = \cos^2 \theta \pi / (k+1)$ for integer k, the entire flow maps U onto S via k crossings. In between, the number of crossings of the two bounding curves are permitted.

(for more details of the derivation and generality of this, see [3]). In this form, the constants $v^{\pm}$ measure the tangents of the angles $\theta^{\pm}$, between the vector fields $\mathbf{f}^{\pm}$ and the z-direction,

$$v^{+} = \frac{\mathbf{f}^{+} \cdot \partial_{\mathbf{x}} y}{\mathbf{f}^{+} \cdot \partial_{\mathbf{x}} z} = \tan \theta^{+}, \qquad v^{-} = \frac{\mathbf{f}^{-} \cdot \partial_{\mathbf{x}} y}{\mathbf{f}^{-} \cdot \partial_{\mathbf{x}} z} = \frac{1}{\tan \theta^{-}},$$

and their product is given by

$$v^{+}v^{-} = \tan \theta^{+} / \tan \theta^{-},$$

which was referred to in the introduction as the 'ratio of tangents'.

5. Dynamics on the switching manifold. In this section, we derive the basic expressions that prescribe sliding and crossing dynamics local to the two-fold.

It is important to note that the singularity is not generically a fixed point of the flow [3, 9]. Therefore, while the local vector field in a general flow is given by the normal form (4.2) in a sufficiently small neighbourhood of the singularity, any solution will leave such a neighbourhood after sufficient time, whereupon higher order terms may become important. Since much of the intrigue surrounding the Teixeira singularity stems from the properties of its normal form alone, this is our sole interest here. Hence the expressions in this section, and the main results derived in section 6, apply strictly to the normal form system (4.2).

5.1. Sliding dynamics. Sliding occurs where the components of $\mathbf{f}^{\pm}$ normal to the switching manifold have opposite signs. Substituting (4.2) into (3.2), the sliding regions in the normal form are given by

$$S = \left\{ (x, y, z) \in \mathbb{R}^3 : x = 0, \ y, z > 0 \right\},$$
$$U = \left\{ (x, y, z) \in \mathbb{R}^3 : x = 0, \ y, z < 0 \right\},$$

where stable and unstable sliding occur respectively (see figure 1.1).

The time derivative (3.3) generates sliding motion in S and U, given by the element of (3.3) that lies tangent to the switching manifold (see [6]), which is

$$\partial_{t^s} \begin{pmatrix} y \\ z \end{pmatrix} = \frac{z}{y+z} \begin{pmatrix} 1 \\ v^+ \end{pmatrix} + \left(1 - \frac{z}{y+z}\right) \begin{pmatrix} v^- \\ 1 \end{pmatrix}$$

(5.1)
$$= \frac{1}{y+z} \begin{pmatrix} z + yv^- \\ y + zv^+ \end{pmatrix}.$$

This is undefined at the singularity, where $y = z = 0$. A local phase portrait can be obtained, however, by neglecting the singular prefactor $1/(y+z)$, and considering the planar vector field

$$\begin{pmatrix} z + yv^- \\ y + zv^+ \end{pmatrix},$$

which has a linear equilibrium at the origin. The trace $(v^+ + v^-)$ and determinant $(v^+v^- - 1)$ of this vector field's Jacobian derivative classify the equilibrium as a focus, node, or saddle. Re-inserting the prefactor yields the local phase portraits in figure 3.1(b), which have appeared in varying forms in [3, 6, 9, 13]. These are not of concern here and are recalled only for completeness.

5.2. Crossing dynamics. The flow crosses through the switching manifold when the components of $\mathbf{f}^\pm$ normal to $x = 0$ have the same sign. Substituting (4.2) into (3.1), the crossing regions in the normal form are given by

$$C^+ = \left\{(x, y, z) \in \mathbb{R}^3 : x = 0, \ y < 0 < z\right\},$$
$$C^- = \left\{(x, y, z) \in \mathbb{R}^3 : x = 0, \ z < 0 < y\right\},$$

where the flow crosses in the positive or negative x directions respectively. The flow outside $x = 0$ is comprised of arcs given by

(5.2) $\qquad (x, y, z) = \begin{cases} \left(\frac{1}{2}(y_0^2 - y^2), y, z_0 + v^+(y - y_0)\right) & \text{for} \quad |y| < |y_0|, \\ \left(\frac{1}{2}(z^2 - z_0^2), y_0 + v^-(z - z_0), z\right) & \text{for} \quad |z| < |z_0|, \end{cases}$

where each arc leaves the switching manifold from coordinates $(0, y_0, z_0)$, and travels through $x > 0$ returning to $(0, -y_0, z_0 - 2v^+y_0)$, or through $x < 0$ returning to $(0, y_0 - 2v^-z_0, -z_0)$ through $x < 0$.

Letting $\mathbf{y}$ denote a two-dimensional column vector with components (y, z), we can thus define a pair of maps, $\phi^\pm$, that take any point $\mathbf{y}_m$ to its first return coordinate $\mathbf{y}_{m+1}$ on $x = 0$, given by

(5.3) $\qquad \mathbf{y}_{m+1} = \phi^+(\mathbf{y}_m) = B^+\mathbf{y}_m, \qquad B^+ = \begin{pmatrix} -1 & 0 \\ -2v^+ & 1 \end{pmatrix},$

(5.4) $\qquad \mathbf{y}_{m+1} = \phi^-(\mathbf{y}_m) = B^-\mathbf{y}_m, \qquad B^- = \begin{pmatrix} 1 & -2v^- \\ 0 & -1 \end{pmatrix}.$

The maps $\phi^\pm$ obey

(5.5) $\qquad \phi^+ : U \cup C^+ \mapsto S \cup C^-, \qquad \phi^- : U \cup C^- \mapsto S \cup C^+.$

The domain of $\phi^\pm$ and range of $\phi^\mp$ overlap on $C^\pm$, on which we can compose ϕ^+ and ϕ^- to define second return maps

(5.6) $\qquad \mathbf{y}_{m+2} = \phi^- \circ \phi^+(\mathbf{y}_m) = A^+\mathbf{y}_m, \qquad A^+ = B^-B^+,$

(5.7) $\qquad \mathbf{y}_{m+2} = \phi^+ \circ \phi^-(\mathbf{y}_m) = A^-\mathbf{y}_m, \qquad A^- = B^+B^-,$

such that

$$(5.8) \qquad \phi^- \circ \phi^+ : U \cup C^+ \mapsto S \cup C^+, \quad \phi^+ \circ \phi^- : U \cup C^- \mapsto S \cup C^-.$$

These second returns maps have been studied in various forms in [6, 9, 12]. The solutions to the difference equations $\mathbf{y}_m = A^\pm \mathbf{y}_{m-2}$ have not, however, been studied explicitly. They are clearly given by

$$(5.9) \qquad \mathbf{y}_{2m} = (\phi^- \circ \phi^+)^m (\mathbf{y}_0) = (A^+)^m \mathbf{y}_0,$$

$$(5.10) \qquad \mathbf{y}_{2m} = (\phi^+ \circ \phi^-)^m (\mathbf{y}_0) = (A^-)^m \mathbf{y}_0,$$

and a little trigonometry using the substitution $v^+ v^- = \cos^2 \theta$ provides

$$(5.11) \qquad (A^\pm)^m = \frac{\sin[2m\theta]}{\sin 2\theta} A^\pm - \frac{\sin[2(m-1)\theta]}{\sin 2\theta} \mathcal{I},$$

where $\mathcal{I}$ denotes the 2×2 identity matrix.

Two properties of the maps $\phi^\pm$ were exploited in [9] to simplify the crossing map. First, the expressions in (5.3) and (5.4) are similar up to the transformation

$$(5.12) \qquad (y, z, v^\pm) \mapsto (z, y, v^\mp).$$

It is therefore sufficient to study the map in (5.9), and infer the corresponding results for (5.10) (or vice versa) by applying the transformation (5.12).

The second property to be exploited is that ϕ^+ and ϕ^- map straight lines through the singularity to each other. It is therefore sufficient to study the angles of points relative to the folds $y = 0$ and $z = 0$, as the matrices $A^\pm$ rotate them around the singularity. Given a point $\mathbf{y}_i$ with components (y_i, z_i), we define its tangent relative to the folds by

$$(5.13) \qquad T_{2m} = \frac{z_{2m}}{y_{2m}}, \qquad T_{2m+1} = \frac{y_{2m+1}}{z_{2m+1}}, \qquad m \in \mathbb{Z},$$

depending on whether i is even ($i = 2m$) or odd ($i = 2m+1$). Then T_m is positive for points $\mathbf{y}_m$ in the sliding regions ($yz > 0$), negative in the crossing regions ($yz < 0$), and either zero or infinite on the folds ($yz = 0$). We thus denote the sets of tangent values T of points in U, S and $C^\pm$, by

$$(5.14) \qquad T_U = T_S = (0, \infty), \qquad T_{C^+} = T_{C^-} = (-\infty, 0).$$

Substituting (5.6)-(5.7) into (5.13), we find that the tangents T_i map as

$$(5.15) \qquad T_{2m+2} = \left(T_{2m} - 2v^+ \right) / \left(1 + 2v^- T_{2m} - 4v^+ v^- \right),$$

$$(5.16) \qquad T_{2m+1} = \left(T_{2m-1} - 2v^- \right) / \left(1 + 2v^+ T_{2m-1} - 4v^+ v^- \right).$$

These second return 'tangent maps' were studied in [9], but again, their solutions as difference equations have not been studied explicitly. Substituting in (5.9)-(5.11), the solutions are found to be given by

$$(5.17) \qquad T_{2m} = \frac{v^+ - T_0 G_m(\theta)}{2v^+ v^- - G_m(\theta) - v^- T_0},$$

(with a similar equation for T_{2m+1} following by (5.12)), using again the quantity $\theta = \arccos \sqrt{v^+ v^-}$ as in (5.11), and introducing the function

$$(5.18) \qquad G_m(\theta) = \frac{\sin[(2m-1)\theta]}{\sin[2m\theta]} \cos \theta.$$

The tangent map $T_0 \mapsto T_{2m}$ given by (5.17) is the main focus of this paper.

6. Structure of the region $v^{\pm} < 0$, $v^+ v^- < 1$. In this section we prove the Theorem and Corollary from section 3. We assume throughout this section that $v^{\pm}$ are negative and $v^+ v^- < 1$. We will derive results that are exact for the normal form (4.2), and more generally hold in a small enough neighbourhood of the singularity.

The theorem is proven by considering how U maps under the action of ϕ^+ and ϕ^-. Without loss of generality we apply ϕ^+ to a point $\mathbf{y}_0 \in U$ (corresponding results for ϕ^- applied to $\mathbf{y}_0 \in U$ are given by the similarity transformation (5.12)). The subsequent orbit consists of crossing points $\mathbf{y}_1, \mathbf{y}_3, ... \mathbf{y}_{m-1} \in C^-$ and $\mathbf{y}_2, \mathbf{y}_4, ... \mathbf{y}_{m-2} \in C^+$ for some integer m, following the convention in [9] that even iterates $\mathbf{y}_{2m}$ lie in the domain of ϕ^+, while odd iterates $\mathbf{y}_{2m+1}$ lie in the domain of ϕ^-. We then have two cases: either $\mathbf{y}_{2m} \in S$, giving an orbit with an odd number of crossings $k = 2m-1$, or $\mathbf{y}_{2m} \in C^+$ and $\mathbf{y}_{2m+1} \in S$, giving an orbit with an even number of crossings $k = 2m$.

We find that, for certain values of the product $v^+ v^-$, the boundaries of U are mapped exactly onto the boundaries of S, and take the same number of crossings (the number of iterates in $C^{\pm}$) to do so. By implication since the maps $\phi^{\pm}$ are linear, all points in U are then mapped into S via the same number of crossings.

Proof of Theorem 3. Let $v^+ v^- = \cos^2 \frac{\pi}{k+1}$ where k is an integer, and let $\pi_k = \frac{\pi}{k+1}$. If $\mathbf{y}_0$ lies on the boundary of U then $T_0 = 0$ or $T_0 = \infty$, then a little algebra gives the tangent of a subsequent point $\mathbf{y}_{2m}$ as

$$(6.1) \qquad T_{2m}|_{T_0=0} = \frac{\sin[2m\pi_k]\cos\pi_k}{\sin[(2m+1)\pi_k]v^-} = \frac{1}{v^-} G_{m+\frac{1}{2}}(\pi_k),$$

$$(6.2) \qquad T_{2m}|_{T_0=\infty} = \frac{\sin[(2m-1)\pi_k]\cos\pi_k}{\sin[2m\pi_k]v^-} = \frac{1}{v^-} G_m(\pi_k).$$

Let us now take a point $\mathbf{y}_0 \in U$ with tangent $T_0 \in T_U$, and consider the map $\mathbf{y}_0 \mapsto \mathbf{y}_{2m} = (\phi^- \circ \phi^+)^m(\mathbf{y}_0)$ which sends $T_0 \mapsto T_{2m}$.

Assuming $k \geq 2$, we must consider two cases:

- If k is odd let $k = 2m-1$, then if $\mathbf{y}_0$ lies on the boundary of U, by (6.1)-(6.2) the point $\mathbf{y}_{2m} = (\phi^- \circ \phi^+)^m(\mathbf{y}_0)$ has tangent $T_{2m}|_{T_0=0} = 0$ or $T_{2m}|_{T_0=\infty} = \pm\infty$ and hence lies on the boundary of S. Since the map is linear this implies that $\mathbf{y}_{2m} = (\phi^- \circ \phi^+)^m(\mathbf{y}_0) \in S$ for any $\mathbf{y}_0 \in U$. By applying (5.15)-(5.16), the iterate $\mathbf{y}_{2m-1}$ has tangent $T_{2m-1} \in (-\infty, 2v^-) \subset T_{C^-}$, and is therefore the last in a sequence of crossing points $\mathbf{y}_{1,3,...,2m-1} \in C^-$ and $\mathbf{y}_{2,4,...,2m-2} \in C^+$, which number $2m-1$ in total; see figure 6.1(ii).
- If k is even let $k = 2m$, then for a point $\mathbf{y}_0$ on the boundary of U, (6.1) and (6.2) give $T_{2m}|_{T_0=0} = \pm\infty$ and $T_{2m}|_{T_0=\infty} = 2v^+$, and therefore by linearity, $\mathbf{y}_{2m}$ belongs to a sequence of crossing points $\mathbf{y}_{1,3,...,2m-1} \in C^-$ and $\mathbf{y}_{2,4,...,2m} \in C^+$. One further application of ϕ^+ sends $T_{2m} \in (-\infty, 2v^+)$ to $T_{2m+1} \in (0, \infty) = T_S$, so the same map sends the boundaries of U to the boundaries of S, and any $\mathbf{y}_0 \in U$ to $\mathbf{y}_{2m+1} = \phi^+ \circ (\phi^- \circ \phi^+)^m(\mathbf{y}_0) \in S$. Thus there are $2m$ crossing points in total; see figure 6.1(i).

In both cases the entire neighbourhood of the singularity consists of orbits that connect U to S via a number of crossings $k = 2m$ or $k = 2m-1$, where k is fixed by the quantity $v^+ v^- = \cos^2 \frac{\pi}{k+1}$. Finally, applying the similarity transformation (5.12), which reflects the topology in figure 6.1 in the line $y = z$, trivially yields the same result when ϕ^- instead of ϕ^+ is applied first on U. $\square$

Proof of Corollary 4. In the theorem above, the boundaries of U map exactly onto the boundaries of S, and $v^+ v^- = \cos^2 \frac{\pi}{k+1}$ where k is an integer. An immediate
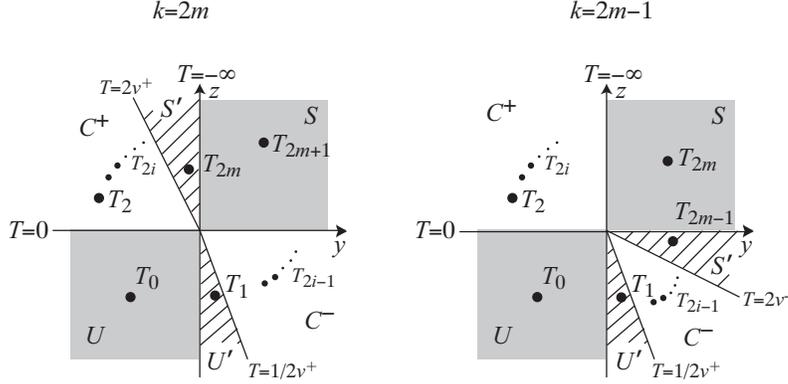
Fig. 6.1. Figure showing: U is the domain of T_0, $U' = \phi^+(U) = (-\infty, 1/2v^+)$ is the region where the first crossing occurs. $S' = (2v^\pm, 0)$ is the region where the last crossing occurs, and is given by $\phi^+(S') = S$ in the left figure, and $\phi^-(S') = S$ in the right figure. There are $k = 2m$ crossings in the left figure and $k = 2m - 1$ in the right, for integer m and $k \geq 2$.

consequence of this is that if $v^+v^- = \cos^2 \frac{\pi}{r+1}$ for non-integer r, then the number of crossing points in the flow can only take the integer values immediately either side of r. To prove this explicitly we consider the orbits that map from inside U to the boundary of S, and from the boundary of U to the interior of S. When these orbits are perturbed they undergo a change in the number of crossing points they contain: if we move from a point $\mathbf{y}_i$ with $T_i > 0$ to one with $T_i < 0$ at the boundary of U, it changes from a starting point in U, to a crossing point in C^+. Thus immediately we have that the number of crossing points increases by one as we go from an orbit with $T_0 \in T_U$ to a nearby orbit with $T_0 \in C^+$, passing through $T_0 = 0$.

It remains to consider orbits that are mapped onto the boundaries of S. Let us assume the zeroth iterate $\mathbf{y}_0$ to be either the start point of an orbit such that $\mathbf{y}_0 \in U$, or to be the first crossing point of an orbit such that $\mathbf{y}_0 = \phi^-(\mathbf{y}_{-1}) \in C^+$ for some $\mathbf{y}_{-1} \in U$. In the first case we have $T_0 \in T_U$, and in the second case, applying (5.3)-(5.4) gives $T_0 \in (1/2v^-, 0)$, recalling that v^- is negative. Likewise, we will assume that some later iterate $\mathbf{y}_i$ is either the end point $\mathbf{y}_i \in S$, or the last crossing point $\mathbf{y}_i \in C^+$ such that $\mathbf{y}_{i+1} = \phi^+(\mathbf{y}_i) \in S$. In the first case $T_i \in T_S$, and in the second case (5.3)-(5.4) gives $T_i \in (-\infty, 2v^+)$, recalling that v^+ is negative. We refer to a *complete orbit* as having a starting point $\mathbf{y}_0$ or $\mathbf{y}_{-1}$ in U, and an endpoint $\mathbf{y}_i$ or $\mathbf{y}_{i+1}$ in S, for some i.

Let us now find the value of T_0 for which T_i lies on the boundary of T_S, where $\mathbf{y}_i$ changes from a crossing point to an end point. Solving $T_{2m}|_{T_0} = 0$ and $T_{2m}|_{T_0} = \pm\infty$ from (5.17) for some integer m, we find

$$
\begin{array}{ll}
T_{2m}|_{T_0} = 0 & \Rightarrow \quad T_0 = \Gamma_m, \\
T_{2m}|_{T_0} = \pm\infty & \Rightarrow \quad T_0 = \Gamma_{m+\frac{1}{2}},
\end{array}
\quad \text{where} \quad \Gamma_m = \frac{v^+}{G_m(\theta)},
$$

recalling that $\theta = \arccos \sqrt{v^+v^-}$ by definition. Now let θ be equal to $\pi_r = \frac{\pi}{r+1}$ for some $r > 0$, and assume that $k < r < k+1$. Let us assume k is odd and let $k = 2m-1$ for some integer m. For the quantity Γ_m it follows that

$$
(6.3) \qquad\qquad \frac{1}{2v^-} < \Gamma_m < 0 < \Gamma_{m+\frac{1}{2}}.
$$

Recall that we allow either $T_0 \in (1/2v^-, 0) \subset T_{C^+}$ or $T_0 \in (0, \infty) = T_U$. Then (6.3)
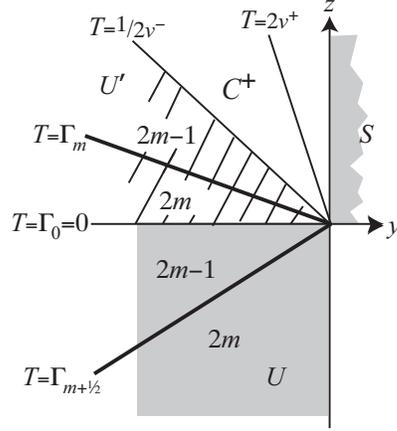
FIG. 6.2. Number of crossings for $2m - 1 < r < 2m$ is $k = 2m$ or $k = 2m - 1$, $m \in \mathbb{Z}$, alternating as the iterate T_0 crosses the tangent values $T_{\delta k}$. To obtain the case $2m < r < 2m + 1$ just substitute m with $m + \frac{1}{2}$.

partitions this range of T_0 values into four different regions:

- if $T_0 \in (\frac{1}{2v^-}, \Gamma_m) \subset T_{C+}$ then $T_{2m-2} \in (-\infty, 2v^+) \subset T_{C+}$ from (5.17). Moreover $\mathbf{y}_0 = \phi^-(\mathbf{y}_{-1})$ for some $\mathbf{y}_{-1} \in U$, and $\phi^+ \circ (\phi^- \circ \phi^+)^{m-1}(\mathbf{y}_0) \in S$, so the complete orbit $\mathbf{y}_{-1} \mapsto \phi^+ \circ (\phi^- \circ \phi^+)^{m-1}(\mathbf{y}_0)$ has $2m - 1$ crossing points $\mathbf{y}_{0,1,\dots,2m-2} \in C^\pm$;
- if $T_0 \in (\Gamma_{m+\frac{1}{2}}, 0) \subset T_{C+}$ then $T_{2m} \in (0, \infty) = T_S$ from (5.17). Moreover $\mathbf{y}_0 = \phi^-(\mathbf{y}_{-1})$ for some $\mathbf{y}_{-1} \in U$, so the complete orbit $\mathbf{y}_{-1} \mapsto (\phi^- \circ \phi^+)^{m-1}(\mathbf{y}_0)$ has $2m$ crossing points $\mathbf{y}_{0,1,\dots,2m-1} \in C^\pm$;
- if $T_0 \in (0, \Gamma_{m+\frac{1}{2}}) \subset T_U$ then $T_{2m} \in (0, \infty) = T_S$ from (5.17), so the complete orbit $\mathbf{y}_0 \mapsto (\phi^- \circ \phi^+)^m(\mathbf{y}_0)$ has $2m - 1$ crossing points $\mathbf{y}_{1,\dots,2m-1} \in C^\pm$;
- if $T_0 \in (\Gamma_{m+\frac{1}{2}}, \infty) \subset T_U$ then $T_{2m} \in (-\infty, 2v^+) \subset T_{C+}$ from (5.17), and moreover $\phi^+ \circ (\phi^- \circ \phi^+)^m(\mathbf{y}_0) \in S$, so the complete orbit $\mathbf{y}_0 \mapsto \phi^+ \circ (\phi^- \circ \phi^+)^m(\mathbf{y}_0)$ has $2m$ crossing points $\mathbf{y}_{1,\dots,2m+1} \in C^\pm$.

On the bounds between these four cases, T_0 maps onto the boundary of T_S by (6.3). If k is even we instead let $k = 2m$, and the corresponding result is found trivially by substituting $m \mapsto m + \frac{1}{2}$ into the cases above. Finally, we have assumed that ϕ^+ is applied first, and the similarity transformation (5.12) gives the corresponding values $T = 0$ and $T = \Gamma_{(k+1)/2} = v^-/G_{(k+1)/2}(\pi_r)$ when ϕ^- is applied first. In each case the number of crossings changes between k and $k + 1$, giving part 1 of the corollary, and the change takes place either at $T = 0$ or at $T = \Gamma_{(k+1)/2} = v^\pm/G_{(k+1)/2}(\pi_r)$, giving part 2 of the corollary. $\square$

As a remark, Theorem 3 shows that the singularity is topologically unstable when $v^+v^- = \cos^2 \frac{\pi}{k+1}$ for integer k, since the flow maps the boundaries of U exactly onto to the boundaries of S. The corollary shows that the intervening cases, when $v^+v^- = \cos^2 \frac{\pi}{r+1}$ for non-integer r, are topologically stable, since the boundaries of U map into the interior of S, and the same number of crossings applies to open intervals of starting points with tangents T_0.

7. Examples. To illustrate the theorem, we simulate the normal form system obtained by substituting (4.2) into (4.1).

In figure 7.1 we take $v^+ = -1$ and $v^- = -0.7$. In the Corollary to Theorem

3, where we let $v^+v^- = \cos^2 \frac{\pi}{r+1}$, we therefore have $r = 4.42$. Hence $4 < r < 5$, implying that the flow can cross either $k = 4$ or $k + 1 = 5$ times between U and S, corresponding to $m = 5/2$ in figure 6.2. Two orbits are shown in figure 7.1, with initial points $\mathbf{y}_0' = (-0.81, -0.59) \in U$ and $\mathbf{y}_0 = (-0.16, -0.99) \in U$, with tangents $T_0' \in (v^+/G_3, \infty)$ and $T_0 \in (0, v^+/G_{5/2}(\arccos \sqrt{v^+v^-}))$, which exhibit four and five crossing respectively. The flow from a point in U can depart the switching manifold into $h > 0$ or $h < 0$, or slide on $h = 0$; to illustrate the corollary we select only the former of these, by perturbing the initial points slightly above U with $x = 10^{-5}$.
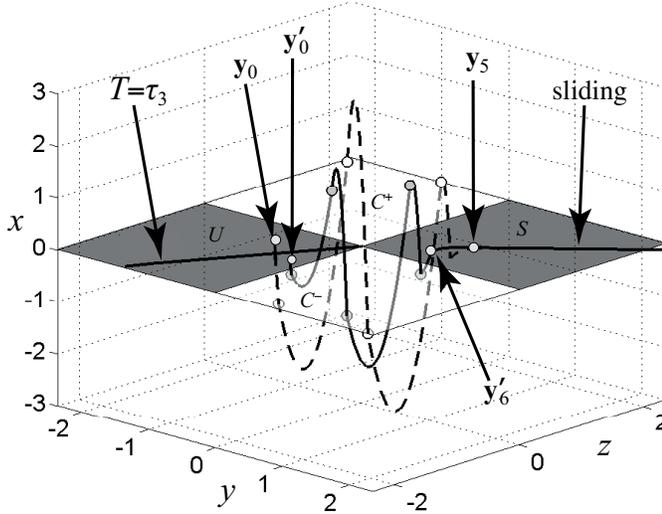

Fig. 7.1. The Teixeira singularity with $v^+v^- = 0.7$. Two orbits with initial points $\mathbf{y}_0$ and $\mathbf{y}_0'$ are shown (dotted and full respectively), winding around from the unstable sliding region U, through the crossing regions $C^\pm$, to the stable reaching the sliding region S. The line with tangent $T = \Gamma_3 = -1/G_3(\arccos \sqrt{0.7})$ is shown in U. The continuation of the orbits into stable sliding is also shown in S.

In figure 7.2 we take $v^+ = -1$ and $v^- = -0.998$, then in the Corollary to Theorem 3 we have $r = 69.2$, hence $69 < r < 70$, implying that the flow should exhibit either 69 or 70 crossing between U and S. A single orbit is depicted, with an initial point $\mathbf{y}_0 = (\cos(3\pi/4), \sin(3\pi/4))$, and undergoes 70 crossings between the sliding regions. (Again the initial point is perturbed slightly above U by giving it an initial x coordinate of 10^{-5}).

As we increase v^+v^- further towards unity (simulations not shown), the path of this orbit remains similar, but its number of crossings tends to infinity, until eventually a pair of invariant cones are born enclosing the regions U and S, described as the *nonsmooth diabolo* bifurcation in [9]. An important point can be made here regarding the interpretation of the normal form. If we instead simulate a non-normal form system, perhaps by adding nonlinear terms, the normal form dynamics will still be found in a sufficiently small neighbourhood of the singularity. If x, y, z, are too large then the statements of crossing numbers may be inaccurate. In particular in the case of infinite crossings (Theorem 2(iii)), the variables *always* become large eventually in forward or backward time, non-local terms take over to augment the normal form behaviour, so the phrase 'infintely many crossing' may no longer hold.

8. Closing remarks. It has been nearly half a century since Filippov described how to solve a discontinuous differential equation [5], and half that since his work [6]
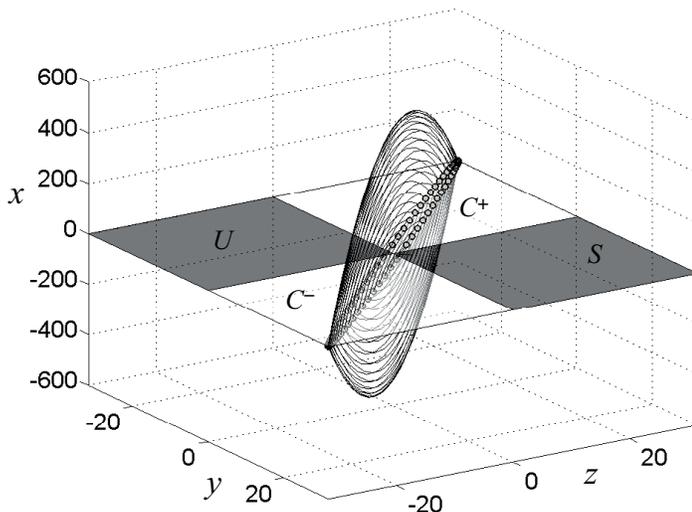
FIG. 7.2. The Teixeira singularity with $v^+v^- = 0.998$. A single orbits is shown, winding around the singularity from U to S, via 70 crossings in the regions $C^\pm$.

raised the problem of the stability of the two-fold singularity. The case where the local flow curves towards the switching manifold on both sides, known as the Teixeira singularity, can now be summarized in Theorems 1 to 3 in section 3. As Filippov stated in [6], there are infinitely many different topological classes of this singularity. Within these classes, however, the topology is structurally stable. Only for $v^+v^- \lesssim 1$, when v_+ and v^- are negative, are these classes infinitely crowded, such that a small perturbation of the system yields a class where the flows rotates a different number of times around the singularity. The precise manner in which this occurs is left to future work.

The different local classes of the Teixeira singularity are identified by a single quantity, called here v^+v^-, which quantifies the discontinuity in the flow's direction at the singularity. The cases are distinguished by the number of crossings that the flow makes between visits to the sliding regions. For a given set of parameters, if the number of crossings is finite, then across the whole flow it can differ only by one. As the parameters vary, bifurcations occurs between different classes in which the two allowed crossing numbers change incrementally.

These bifurcations occur when $v^+v^- = \cos^2 \frac{\pi}{k+1}$ and k is an integer, whereupon the boundaries of unstable and stable sliding are mapped exactly onto each other by the flow. Clearly this scenario is topologically unstable and, at these values, the role of higher order terms becomes important to break the degeneracy. For the case $k \to \infty$ this was studied in [3]. For the cases described in this paper, when k is finite, one expects that higher order terms will perturb the bifurcation curves $v^+v^- = constant$, without altering the dynamics (in particular the range of crossing numbers exhibited by the flow for nearby parameters) significantly.

Not wishing to extinguish the two-fold's ability to confound, there remain certain peculiarities within the classification made in section 3. It has been pointed out by Jesus Enrique Achire Quispe at the University of Campinas that, for certain parameter values, it would seem possible for pairs of orbits to form closed loops if they become connected by sliding segments in both the unstable region U and the stable region S

(figure 8.1(ii)). Simulations of the normal form system suggest this may occur only at $v^+v^- = 1$, but this has not been proven conclusively. Also, for certain parameters, the sliding segment through the singularity can be mapped onto the folds by the crossing dynamics (figure 8.1(iii)). These non-generic scenarios are topologically unstable, but they appear to be of no significance for the dynamics along any orbit, and therefore do not feature in the dynamical classification in the present paper. They do, however, contribute to an ongoing conundrum of how to define topological equivalence in nonsmooth systems.
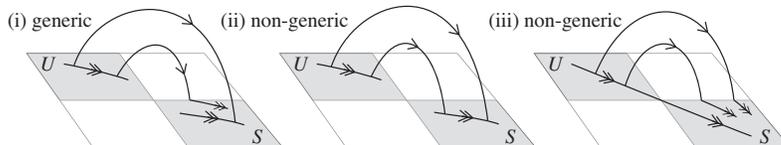

FIG. 8.1. (i) a typical stable topology, (ii) a closed loop formed by sliding and non-sliding segments, (iii) a unique sliding segment through the singularity maps onto a fold. Scenarios (ii)-(iii) represent unstable topologies but have no critical effect on dynamics.

We have derived results here that apply strictly to the normal form, and therefore assume that this approximates the flow in a general system in a neighbourhood of a two-fold singularity. The theory of normal forms, and the coordinate transformations and topological equivalences used to obtain them, is still at a developmental stage in nonsmooth systems. We hope that the pragmatic appoach taken here (and in [3, 9]), of deriving the dynamics of the normal form as a local model, will help guide future study of equivalence, stability, and genericity, in piecewise smooth dynamical systems.

For the cases of two-fold singularity not considered here, where the dynamics curves away from the switching manifold on one or both sides, there always exist directions locally that carry the flow away from the singularity (see for example [3, 6, 13]), and the issue of structural stability is rather more simple. Among the different forms of two-fold, some cases channel the flow between sliding regions, either from stable to unstable or vice versa, and others convey the flow around the singularity without any orbits passing through it. These different cases have a wider role to play in the emerging theory of global dynamics of nonsmooth flows in three or more dimensions (see for example [10]), and their study is ongoing.

REFERENCES

[1] G. Bachar, E. Segev, O. Shtempluck, E. Buks, and S. W. Shaw. Noise induced intermittency in a superconducting microwave resonator. *EPL*, 89(1):17003, 2010.

[2] B. Brogliato. *Impact in mechanical systems - analysis and modelling*, volume 551 of *Lecture Notes in Physics*. Springer-Verlag (New York), 2000.

[3] A. Colombo and M. R. Jeffrey. Non-deterministic chaos, and the two-fold singularity in piecewise smooth flows. *SIAM J. App. Dyn. Sys.*, 10:423–451, 2011.

[4] M. di Bernardo, C. J. Budd, A. R. Champneys, and P. Kowalczyk. *Piecewise-Smooth Dynamical Systems: Theory and Applications*. Springer, 2008.

[5] A. F. Filippov. Differential equations with discontinuous right-hand side. *American Mathematical Society Translations, Series 2*, 42:19–231, 1964.

[6] A. F. Filippov. *Differential Equations with Discontinuous Righthand Sides*. Kluwer Academic Publ. Dortrecht, 1988.

[7] J.-L. Gouzé and T. Sari. A class of piecewise linear differential equations arising in biological models. *Dynamical Systems*, 17(4):299–316, 2002.

[8] M. R. Jeffrey. Non-determinism in the limit of nonsmooth dynamics. *Physical Review Letters*, 106(254103):1–4, 2011.

[9] M. R. Jeffrey and A. Colombo. The two-fold singularity of discontinuous vector fields. *SIAM Journal on Applied Dynamical Systems*, 8(2):624–640, 2009.

[10] M. R. Jeffrey and S. J. Hogan. The geometry of generic sliding bifurcations. *SIAM Review*, 53(3):505–525, 2011.

[11] Yu. A. Kuznetsov, S. Rinaldi, and A. Gragnani. One-parameter bifurcations in planar Filippov systems. *Int.J.Bif.Chaos*, 13:2157–2188, 2003.

[12] M. A. Teixeira. Stability conditions for discontinuous vector fields. *J. Differ. Equ.*, 88:15–29, 1990.

[13] M. A. Teixeira. Generic bifurcation of sliding vector fields. *J.Math.Anal.Appl.*, 176:436–457, 1993.

[14] V. I. Utkin. Variable structure systems with sliding modes. *IEEE Trans. Automat. Contr.*, 22, 1977.

[15] J. Wojewoda, S. Andrzej, M. Wiercigroch, and T. Kapitaniak. Hysteretic effects of dry friction: modelling and experimental studies. *Phil. Trans. R. Soc. A*, 366:747–765, 2008.

Appendix A.

The Lie derivative is a standard tool appearing in most texts on dynamical systems, however the notation $\partial_{t\pm}$ used in sections 2 and 3 is non-standard. It is therefore worth a few remarks.

The notation $\partial_{t\pm}$ is employed here for two reasons. Firstly, the operators $\partial_{t\pm}$ are sufficient to specify both the piecewise-smooth flow, and most singularities of interest, without having to introduce the vector fields $\mathbf{f}^{\pm}$ explicitly (note that these do not appear until the normal form analysis of section 4).

Secondly, $\partial_{t\pm}$ represents a time derivatve. The Lie derivative with respect to some $\mathbf{f}$ is the directional derivative along $\mathbf{f}$, given by the operator $\mathbf{f} \cdot \partial_{\mathbf{x}}$. In the language of dynamical systems, if $\mathbf{f}$ is taken to be a velocity field $\mathbf{f} = d\mathbf{x}/dt$, then we can write $\mathbf{f} \cdot \partial_{\mathbf{x}} = (d\mathbf{x}/dt) \cdot \partial_{\mathbf{x}} = d/dt$, so the Lie derivative is just the time derivative along a flow with velocity $\mathbf{f}$. There are two ways to avoid explicit dependence on the coordinate system $\mathbf{x}$, either replacing $\mathbf{f} \cdot \partial_{\mathbf{x}}$ with a symbol $\mathcal{L}_{\mathbf{f}}$ (see e.g. [4]), or by letting the symbol $\mathbf{f}$ itself give the Lie derivative when acting on a function, so $\mathbf{f}h = \mathbf{f} \cdot \partial_{\mathbf{x}}h$ (see e.g. [12, 13]). In fact, it is unecessary to explicitly specify either the coordinate system $\mathbf{x}$ or the vector field $\mathbf{f}$, if one *defines* the flow by the derivative '∂' with respect to time t taken along it, hence we use the symbol ∂_t. More specifically, in our piecewise-smooth flow we have two operators $\partial_{t\pm}$, in regions indexed by '$\pm$' denoting the sign of a function h.